



Sulfur and Saccharin Incorporation into Electrodeposited CoFe Alloys: Consequences for Magnetic and Corrosion Properties

Jinnie George, James Rantschler, Sang-Eun Bae,*
Dmitri Litvinov, and Stanko R. Brankovic*^z

Electrical and Computer Engineering Department & Center for Nanomagnetic Systems, University of Houston, Houston, TX 77204-4005, USA

Incorporation of sulfur into 2.4 T CoFe alloys during galvanostatic deposition has been studied. The results indicate that the main source of sulfur in magnetic deposit is saccharin used as an additive in the plating solution. The atomic percent of sulfur in deposit and the sulfur incorporation rate show strong dependence on saccharin concentration in the plating solution. This dependence has pronounced maximum at $C_{\text{sac}} \approx 0.12 \text{ g L}^{-1}$, while for $C_{\text{sac}} \geq 1.5 \text{ g L}^{-1}$ the incorporation rate approaches constant value. A simple physical model is developed to describe the sulfur incorporation as a function of saccharin concentration having an excellent qualitative agreement with experimental data. The corrosion and magnetic properties of the electrodeposited 2.4 T CoFe alloys were found to be the strong function of the sulfur incorporation rate, and these results are discussed within the framework of the proposed sulfur incorporation model.

© 2008 The Electrochemical Society. [DOI: 10.1149/1.2948377] All rights reserved.

Manuscript submitted April 9, 2008; revised manuscript received May 27, 2008. Published July 16, 2008.

The electrodeposition of magnetically soft, high magnetic moment alloys has been extensively used in the manufacturing of magnetic recording heads, microelectromechanical systems (MEMS) and nanoelectromechanical systems (NEMS).¹ The cost effectiveness and facility of implementation have resulted that electrodeposition is now being the main approach used in the fabrication of soft magnetic nanostructures in many emerging fields of nanotechnology. Current research in the electrodeposition of soft magnetic alloys is driven by the need for magnetic alloys with the highest possible magnetic moment² and reliable and easily controlled processes, which can deliver nanosize magnetic structures used as an integral part of devices with critical dimensions below 50 nm.^{3,4} At this scale, the reliability and performance of magnetic devices becomes critically dependent on the properties of the electrodeposited alloys, their stability during different fabrication steps, and their compatibility with other materials used for magnetic device fabrication. These criteria require that the understanding of the phenomena determining the properties of magnetic alloys be further improved in order to define the optimum electrodeposition process to obtain the alloys with desired characteristics.

The development of electrodeposited soft magnetic alloys has gone through several phases in the last three decades. In the very beginning, the alloy of choice was $\text{Ni}_{81}\text{Fe}_{19}$ (Permalloy) with saturation magnetic flux density $B_s = 1 \text{ T}$.⁵ Further development introduced $\text{Ni}_{45}\text{Fe}_{55}$ with 70% higher B_s values⁶ and ternary CoFeNi alloys with lower Ni content and B_s ranging between 1.6 and 2.2 T.^{2,7-9} In recent years, the electrodeposited soft CoFe alloys with the highest magnetic moment on the Slater–Pauling curve of 2.4 T and composition in the range of $\text{Co}_{30-50}\text{Fe}_{70-50}$ were demonstrated as well.^{2,3,10} These alloys certainly represent one of the most promising materials for fabrication of the future magnetic recording heads, MEMS and NEMS devices, and the improvement of their properties is the subject of research efforts in industry and academia as well.

In order to obtain magnetic alloys with lower coercivity, different additives have been used in the plating solutions.^{6-8,10,11} In addition to producing the soft alloys, the common action of additives is expressed through the leveling and brightening of the deposit, improvement of the crystal structure,¹² smaller grain size,^{7,8} and the reduction of the residual stresses.¹³ The last two effects are also important for obtaining ultimately soft 2.4 T CoFe alloys.² The use of additives in the plating solutions results in the incorporation of different amounts of nonmagnetic interstitials and inclusions in the magnetic deposit.^{12,14,15} Entire additive molecules or molecular

fragments can be found in deposit as well.^{16,17} If the amount of the incorporated additives is small, it is generally considered beneficial for the desired magnetic softness.⁸ However, the significant presence of sulfur, metal sulfides, or S-containing organic molecules and fragments, can cause a detrimental deterioration of the magnetic alloy corrosion resistance.^{18,19} The sulfur incorporation into magnetic deposit coming from the saccharin as an additive occurs either via saccharin adsorption-electroreduction or via its physical incorporation during the deposit growth.^{16,17} The first mechanism represents the chemical route responsible for incorporating S-containing molecular fragments and metal sulfides in the deposit,^{14,15,20} whereas the second one represents the incorporation of entire molecules of saccharin having sulfur atom as their integral part.^{16,17} In addition to these two additive-related mechanisms, the physical entrapment of sulfur containing ions (SO_4^{2-} , SO_3^{2-} , ...) cannot be excluded as a source of sulfur in the magnetic deposit. At present, the relative contribution of each of these mechanisms to the overall content of sulfur in the magnetic deposit is unknown. Elucidating the conditions favoring the particular sulfur incorporation route is important for our understanding of the role that sulfur incorporation and additives (saccharin) have on physical properties of the electrodeposited magnetic alloys.

The sulfur incorporation represents a great problem when corrosion properties of electrodeposited 2.4 T CoFe are evaluated.^{21,22} As an illustration, in Fig. 1 the corrosion potential transients for the 2.4 T CoFe alloys obtained from the solution containing saccharin as an additive and sputtered CoFe alloy are presented.²³ As one can see, the corrosion potential of electrodeposited CoFe alloy is measured to be $\approx 0.3 \text{ V}$ more negative than the corrosion potential of the sputtered 2.4 T CoFe alloy (Fig. 1). If these results are translated in the comparative corrosion rates,²⁴ then it can be shown that CoFe alloy obtained from saccharin containing solutions should corrode many times faster than the sputtered ones. This fact has to be attended to when electrodeposited 2.4 T CoFe nanostructures, which are just a few tens of nanometers in their critical dimensions, are considered. A poor alloy corrosion resistance can lead to magnetic nanostructure disintegration and loss in a much shorter time than what is expected for the bulk alloy. Therefore, the design of the optimum plating solution is a challenge that requires a deeper insight into all the effects that additives (saccharin) have on magnetic and corrosion properties of 2.4 T CoFe alloys.

In this paper, the results from our studies of the sulfur incorporation into 2.4 T CoFe magnetic alloys are presented. The sulfur incorporation rate is found to be a strong function of the saccharin concentration in the plating solution (C_{sac}) in the range $0.06 < C_{\text{sac}} < 1.5 \text{ g L}^{-1}$. This dependence has a pronounced maximum $R_S = 1.9 \times 10^{-11} \text{ mol cm}^{-2} \text{ s}^{-1}$ at $C_{\text{sac}} \approx 0.12 \text{ g L}^{-1}$. For C_{sac}

* Electrochemical Society Active Member.

^z E-mail: stanko.brankovic@mail.uh.edu

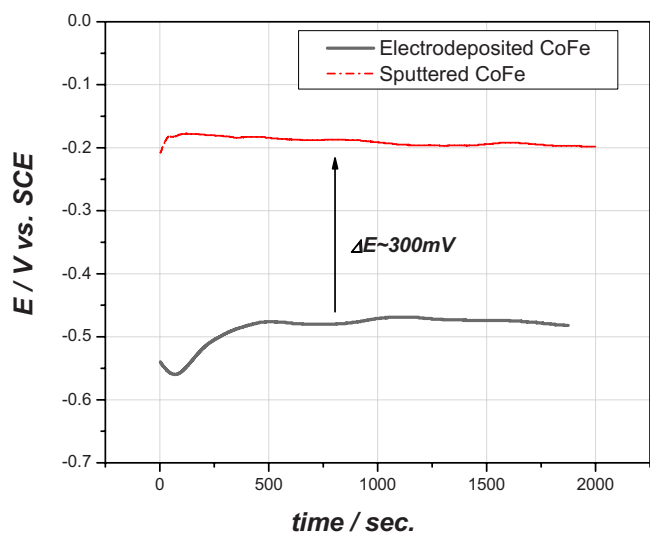


Figure 1. (Color online) The corrosion potential transients for sputtered (dashed) and electrodeposited 2.4 T CoFe alloy (solid line). Test solution: 0.5 M NaCl. Data adopted from Ref. 23.

> 1.5 g L⁻¹, the sulfur incorporation rate decreases slowly toward its minimum value, $R_S \approx 1.0 \times 10^{-11}$ mol cm⁻² s⁻¹, for $C_{sac} \approx 2.5$ g L⁻¹. A simple analytical model is developed to describe sulfur incorporation as a function of saccharin concentration in the plating solution having an excellent qualitative agreement with experimental data. The corrosion properties and coercivity of CoFe alloys are investigated as a function of C_{sac} , and these results are discussed within the framework of the developed analytical model.

Experimental

A standard three-electrode cell configuration with solution volume (V) of 5 L was used to electrodeposit 0.6 ± 0.05 μm thick Co₄₀₋₄₅Fe₆₀₋₅₅ films (further references to CoFe films in this text will denote this composition). The cathodes were rotating Cu disks ($D = 1.7$ cm), and a Co plate was used as an anode. The reference electrode was saturated calomel electrode, and all potentials in this study are quoted with respect to it. The electrodeposition is carried out under galvanostatic control, and solution design and parameters of electrodeposition process are described in Table I. The additive used in the deposition experiments was saccharin with concentration ranging from 0 to 2.5 g L⁻¹. All corrosion measurements were performed in 0.05 M NaCl solution. The composition of the CoFe samples was verified by energy dispersive X-ray spectroscopy. The magnetic properties of the CoFe films were verified using a vibrating sample magnetometer (VSM). The thickness of the CoFe films was determined from scanning electron microscopy images of focused ion beam cross sections and from charge-stripping measurements. After the deposition of CoFe films and verification of their magnetic properties, thickness, and composition, the samples were subjected to wavelength dispersive X-ray spectroscopy (WDS) analysis to determine the amount of incorporated sulfur in the deposit. The experimental data represent the average of at least three

Table I. Plating solution and process parameters.

Solution components (mol · L ⁻¹)		Process parameters	
FeSO ₄	0.1	j	4 mA cm ⁻²
CoSO ₄	0.046	ω	220 rpm
(NH ₄)Cl	0.3	γ	0.12
H ₃ BO ₃	0.4	R_{CoFe}	2.5×10^{-9} mol cm ⁻² s ⁻¹
pH	2.1	T	298 K

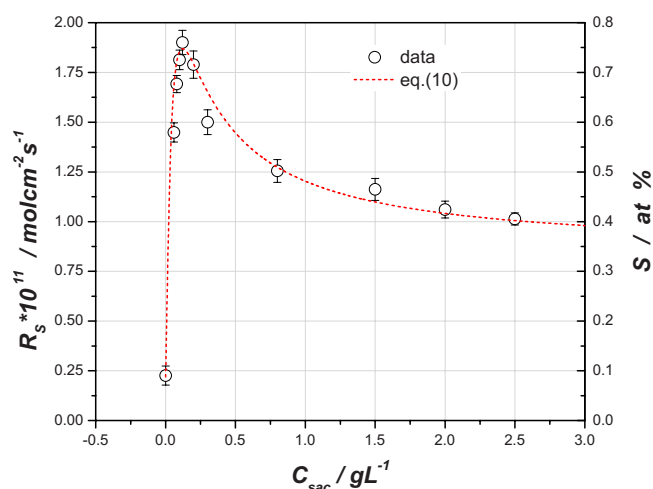


Figure 2. (Color online) The WDS measurements showing atomic percent of S as a function of saccharin concentration in the bath, (right ordinate), and corresponding sulfur incorporation rate (left ordinate) [Eq. 1].

measurements per sample for at least four samples per each concentration of saccharin in the plating solution. The error bars are calculated as the standard deviation of all measurements for samples obtained from a particular concentration of saccharin. The incorporation rate of sulfur [units presented as flux (in moles per centimeters squared per second)] was obtained from the WDS data (S atomic percent) using the following expression

$$R_S = \frac{SR_{CoFe}}{100 - S} \quad [1]$$

Here, $R_{CoFe} = 2.5 \times 10^{-9}$ mol cm⁻² s⁻¹ is calculated from the data presented in Table I using $R_{CoFe} = \gamma j / 2F$.

Results and Discussion

Sulfur incorporation vs C_{sac} .— The results from the WDS analysis of 2.4 T CoFe films deposited from solutions with different C_{sac} are presented in Fig. 2. The importance of C_{sac} is examined through its influence on the incorporation rate of sulfur R_S [Eq. 1 (in moles per centimeters squared per second)] (left ordinate) and on the atomic percent of S in the deposit (right ordinate). For the range of investigated saccharin concentrations, the R_S vs C_{sac} results show a pronounced maximum, resembling the dependence with asymmetric peak shape. The important thing to note in Fig. 2 is that sulfur content and corresponding R_S in the CoFe films is not zero for the samples produced from solutions without saccharin ($C_{sac} = 0$ g L⁻¹). This indicates that saccharin is not the only source of sulfur in the deposit. The addition of small amounts of saccharin (0.06 g L⁻¹) into the plating solution results in a steep increase in R_S of almost seven times (from 0.22×10^{-11} to 1.45×10^{-11} mol cm⁻² s⁻¹). The R_S quickly reaches its maximum (1.9×10^{-11} mol cm⁻² s⁻¹) at $C_{sac} \approx 0.12$ g L⁻¹, and an additional increase of the saccharin concentration of the solution leads to a gradual decrease in R_S . The increase of C_{sac} by more than 10 times, from 0.12 to 1.5 g L⁻¹, results in a decrease of R_S of only $\approx 40\%$. A further increase of the saccharin concentration beyond the 1.5 g L⁻¹ value leads to a very slow decrease of R_S to its minimum of $\approx 1.0 \times 10^{-11}$ mol cm⁻² s⁻¹, obtained from the upper limit of investigated saccharin concentrations ($C_{sac} = 2.5$ g L⁻¹).

R_S vs C_{sac} analytical model.— An analytical model describing the R_S vs C_{sac} dependence is developed by taking into account several assumptions.^{17,23} The first one is that adsorbed saccharin on the CoFe surface is in equilibrium with its solvated phase in the bulk solution, which allows us to use Langmuir adsorption models to describe the coverage of this additive as a function of its concentra-

tion in the solution. This assumption is based on the fact that the total amount of saccharin in the solution is many orders of magnitude larger than its amount incorporated into deposit during electrodeposition, which implies that C_{sac} is const. The potential transient measurements demonstrate that the CoFe electrode potential reaches a steady state within the first 30 s of galvanostatic deposition, which means that $E = \text{const}$, and thus the saccharin coverage, θ , of the CoFe surface is const for 99% of the deposition time.^{17,23}

The second assumption is that, in the concentration range of our experimental data ($0.06 < C_{\text{sac}} < 1.5 \text{ g L}^{-1}$), there are no transport limitations encountered at any time for saccharin arrival at the electrode surface. This assumption is supported by comparison between the calculated diffusion limited flux of saccharin, R_{dif} , with sulfur incorporation rate R_S for each experiment. In this comparative analysis, we assume that each sulfur atom in the deposit is coming from one molecule of saccharin, which is certainly a conservative overestimate since we do see from our data (Fig. 2) that other sources of sulfur exist in the deposit as well. Using the typical literature value for the diffusion coefficient of additives²⁵ ($D_S = 1 \times 10^{-6} \text{ cm}^2 \text{ s}^{-1}$) and the kinematic viscosity of water as $\nu = 0.01 \text{ cm}^2 \text{ s}^{-1}$, the representative estimate of the D_S/δ ratio is calculated to be $0.62 \times 10^{-3} \text{ cm s}^{-1}$ ($D_S/\delta = 0.62 \cdot D_S^{0.67} \omega^{0.5} \nu^{-0.17}$).²⁶ The diffusion limited flux of saccharin can be expressed as $R_{\text{dif}} = (D_S/\delta)C_{\text{sac}}$, and for the lowest concentration of saccharin in our experiments ($C_{\text{sac}} = 0.06 \text{ g L}^{-1} = 3.2 \times 10^{-7} \text{ mol cm}^{-3}$), the diffusion limited flux is calculated to be $1.98 \times 10^{-10} \text{ mol cm}^{-2} \text{ s}^{-1}$. This value is ≈ 14 times greater than the incorporation rate of sulfur measured in corresponding experiment ($R_S = 1.45 \times 10^{-11} \text{ mol cm}^{-2} \text{ s}^{-1}$), which supports the validity of the starting assumption.

The analytical model considers the total rate of sulfur incorporation R_S to be the sum of several contributions coming from different and independently operating incorporation mechanisms described previously. It is important to point out that each of these incorporation mechanisms is introducing sulfur into magnetic deposit in a different form. The sulfur incorporation rate related to sources other than saccharin is marked as R_0 . We assume that $R_0 = \text{const}$ for an entire range of investigated additive concentrations, and its value could be deduced from our experimental data (Fig. 2). For $C_{\text{sac}} = 0 \text{ g L}^{-1}$, the $R_S = 0.22 \times 10^{-11} \text{ mol cm}^{-2} \text{ s}^{-1}$, which means that sulfur incorporation from sources other than saccharin is defined as

$$R_S(C_{\text{sac}} = 0) = R_0 = 0.22 \times 10^{-11} \text{ mol cm}^{-2} \text{ s}^{-1} \quad [2]$$

The electroreduction of saccharin on the growing CoFe surface can be represented as the surface controlled chemical reaction of the first order whose rate is defined in flux units as²⁷

$$r_{\text{ER}} = kC_{\text{sac}}^S \quad [3]$$

Here, the term k represents the reduction rate constant defined in per-second units. The term C_{sac}^S represents the concentration of saccharin adsorbed layer on CoFe surface expressed in [moles per second] units. This term can be further described in terms of saccharin coverage, θ , and the surface concentration of the full saccharin monolayer Γ_{ML} as

$$C_{\text{sac}}^S = \Gamma_{\text{ML}}\theta \quad [4]$$

The incorporation of sulfur into the deposit as a result of electroreduction of saccharin, R_{ER} , can either come via formation of metal sulfides, where reduction of sulfur atom from saccharin is completely achieved (S^{2-}),²⁰⁻²² or it could result in incorporation of partially reduced saccharin fragments where the oxidation state of the sulfur atom could have different values.²¹ In both cases, we assume that the initial step of saccharin reduction to orthotoulene-sulfonamide is the rate-controlling step^{21,22} and, for this reason, the sulfur incorporation rate via electroreduction mechanism is equal to the electroreduction rate of saccharin (Eq. 3) corrected by the dimensionless efficiency factor χ . We introduce the χ factor in order to take into account the possibility that not every atom of sulfur

Table II. The values of constants in Eq. 10 and extracted parameters from the fit.

	Values of the constants in Eq. 10	Extracted parameters from the Eq. 10 fit of the data in Fig. 2	
Γ_{ML}	$3.3 \times 10^{-10} \text{ mol cm}^{-2}$, Ref. 17	b	10.8 L g^{-1}
d_{sac}	$0.8 \times 10^{-7} \text{ cm}$, Ref. 12	$\Delta\nu$	$1.3 \times 10^{-8} \text{ cm s}^{-1}$
R_0	$0.22 \times 10^{-11} \text{ mol cm}^{-2} \text{ s}^{-1}$, Fig. 2	$\chi \cdot k$	0.019 s^{-1}

belonging to the initially electroreduced saccharin molecule gets incorporated into the CoFe deposit. The final expression for R_{ER} reads as

$$R_{\text{ER}} = \chi r_{\text{ER}} = \chi k \Gamma_{\text{ML}} \theta \quad [5]$$

In our previous work,^{17,23} we have shown that physical incorporation of entire saccharin molecules into CoFe deposit can be explained using the simple model based on the interplay between the two phenomena. The first one is the saccharin adsorption on CoFe surface, and the second one is the overgrowth of the adsorbed saccharin molecules by the free CoFe surface. According to this model, the physical incorporation of entire saccharin molecules into a 2.4 T CoFe deposit expressed in units of flux is defined as^{17,23}

$$R_M = \frac{\Gamma_{\text{ML}} \Delta\nu}{d_{\text{sac}}} \theta (1 - \theta) \quad [6]$$

Here, the term $\Delta\nu$ refers to the difference between growth rate of the free CoFe surface and the growth rate of the CoFe surface covered by saccharin molecules. The term d_{sac} represents the diameter of the saccharin molecule.

The total incorporation rate of sulfur into CoFe deposit can be expressed as a sum of the incorporation rates related to all three discussed mechanisms as

$$R_S = R_0 + R_{\text{ER}} + R_M \quad [7]$$

After combining Eq. 2, 5, and 6 with Eq. 7, the complete model of sulfur incorporation expressed in terms of saccharin coverage is presented as

$$R_S = R_0 + \chi k \Gamma_{\text{ML}} \theta + \frac{\Gamma_{\text{ML}} \Delta\nu}{d_{\text{sac}}} \theta (1 - \theta) \quad [8]$$

If the saccharin adsorption is described in terms of Langmuir formalism²⁸

$$\theta = \frac{bC_{\text{sac}}}{1 + bC_{\text{sac}}} \quad [9]$$

then the final form of the sulfur incorporation rate, R_S , as a function of saccharin concentration reads as

$$R_S = R_0 + \chi k \Gamma_{\text{ML}} \frac{bC_{\text{sac}}}{1 + bC_{\text{sac}}} + \frac{\Gamma_{\text{ML}} \Delta\nu}{d_{\text{sac}}} \frac{bC_{\text{sac}}}{(1 + bC_{\text{sac}})^2} \quad [10]$$

In this expression, the only unknowns are b as the saccharin adsorption constant, $\Delta\nu$ and the product χk . The values of other constants are known from the literature ($d_{\text{sac}} \approx 0.8 \times 10^{-7} \text{ cm}$)¹² or they can be easily calculated ($\Gamma_{\text{ML}} \approx 3.3 \times 10^{-10} \text{ mol cm}^{-2}$)¹⁷ or determined experimentally ($R_0 = 0.22 \times 10^{-11} \text{ mol cm}^{-2} \text{ s}^{-1}$). Equation 10 is used to fit our results in Fig. 2 [dashed line ($0.06 < C_{\text{sac}} < 2.5 \text{ g L}^{-1}$)]. The values of parameters χk , $\Delta\nu$, and b extracted from this fit are presented in Table II. As can be seen, our model succeeds in qualitatively explaining our experimental results very well. The extracted values of the parameters χk , $\Delta\nu$, and b from the fit are such that the incorporation rate of sulfur described by Eq. 10 is always lower than the diffusion limited flux of saccharin toward the CoFe surface ($R_{\text{dif}} = 0.62 \times 10^{-3} \times C_{\text{sac}}$ in moles per centimeters squared per second). This fact ensures that the validity of our model can be extended to the $C_{\text{sac}} \rightarrow 0 \text{ g L}^{-1}$ limit, as shown in Fig. 2.

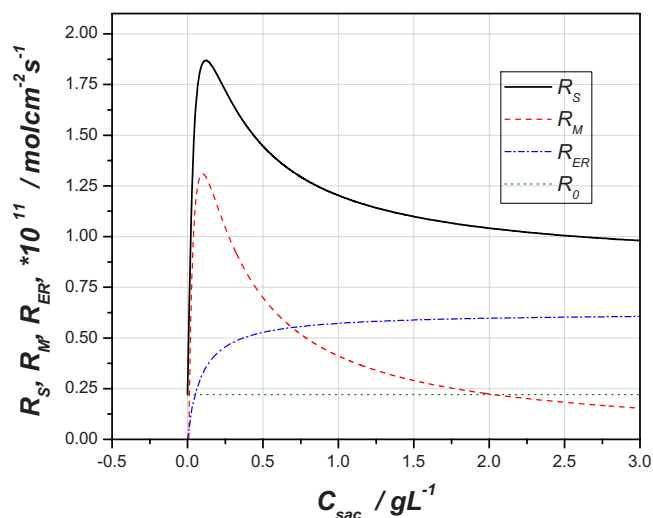


Figure 3. (Color online) The incorporation rate of sulfur via physical incorporation of saccharin molecules (R_M , dashed line), saccharin electroreduction (R_{ER} , dashed dotted line), and from nonsaccharin-related sources (R_0 , dotted line) as a function of C_{sac} . The rates are calculated using data from Table II. The total sulfur incorporation rate is also shown for comparison (R_S).

The mathematical nature of our model allows us to perform a deconvolution of the sulfur incorporation rate on separate contributions of each incorporation mechanism. This analysis is shown in Fig. 3, where the incorporation rate coming from each mechanism is calculated using the values of the parameters from Table II. It is evident that the major contribution to the shape of R_S vs C_{sac} dependence is coming from the R_M vs C_{sac} functionality. For $0 \leq C_{sac} \leq 0.7 \text{ g L}^{-1}$, the dominant sulfur incorporation mechanism is the physical entrapment of saccharin molecules ($R_M > R_{ER}$). The dominant form of sulfur in the CoFe deposit in this concentration range is as a part of the saccharin molecule. However, when $C_{sac} > 0.7 \text{ g L}^{-1}$, the dominant sulfur incorporation mechanism is saccharin electroreduction ($R_{ER} > R_M$). In our previous study,^{17,23} we found that molecular fragments of saccharin were one or more orders of magnitude less populated in the 2.4 T CoFe films than the saccharin molecules. Because of that, it is a plausible assumption that for C_{sac} range where $R_{ER} > R_M$, the dominant form of sulfur in 2.4 T CoFe deposit is as a part of metal sulfides rather than as a part of other saccharin related molecular fragments. The one more important suggestion of our model is that R_M vs C_{sac} as well as R_{ER} vs C_{sac} are the functions that have asymptotes for $C_{sac} \rightarrow \infty$ ($R_M \rightarrow 0$ and $R_{ER} \rightarrow \chi k \Gamma_{ML} = 0.625 \times 10^{-11} \text{ mol cm}^{-2} \text{ s}^{-1}$). This means that R_S is decreasing asymptotically for increasing values of C_{sac} . Therefore, the experimentally observed very slow decrease of sulfur incorporation rate for $C_{sac} > 1.5 \text{ g L}^{-1}$, according to our model, should never lead to values lower than the value of R_S asymptote defined as $R_0 + \chi k \Gamma_{ML} = 0.845 \times 10^{-11} \text{ mol cm}^{-2} \text{ s}^{-1}$.

Coercivity vs C_{sac} and R_S .—In order to explore the effect of sulfur incorporation on the resultant coercivity of 2.4 T CoFe alloys, the deposited 2.4 T CoFe films were subjected to VSM measurements. The results are presented in Fig. 4A as coercivity (H_c) vs the content of saccharin in the plating solution. This dependence is quite different from what has been reported previously for the CoNiFe and NiFe films.^{12,29} Rather than observing a monotone decrease of H_c (NiFe alloys²⁹) or $H_c \approx \text{const}$ (CoNiFe¹²) for increasing C_{sac} , in the case of 2.4 T CoFe films, a more complex H_c vs C_{sac} dependence was observed. As expected, the largest values of coercivity are measured for CoFe films obtained from solution without saccharin. Small additions of this additive results in significant decreases of the deposit coercivity, which has the lowest value ($H_c = 43 \text{ Oe}$) for the CoFe films produced from solution containing 0.12 g L^{-1} of

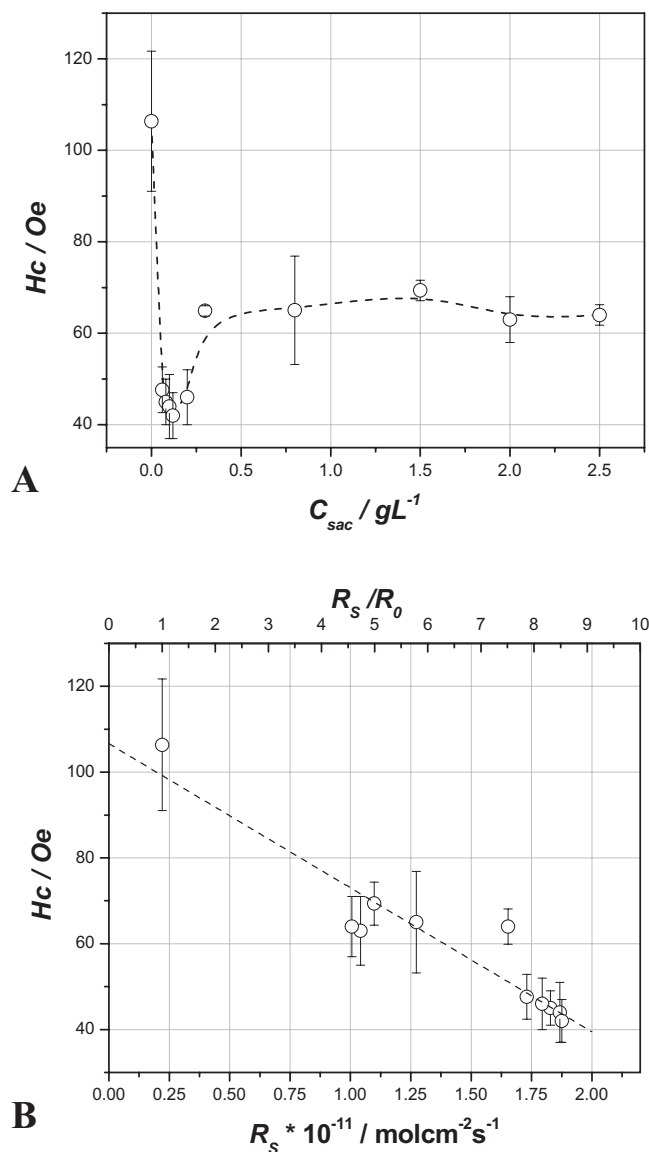


Figure 4. (A) Coercivity of 2.4 T CoFe alloys as a function of saccharin concentration in the plating solution. (B) Coercivity of 2.4 T CoFe alloys as a function of sulfur incorporation rate (bottom axes) and ratio between R_S/R_0 (top axes).

saccharine. Further increasing the saccharin concentration yields CoFe films with higher H_c values. For the CoFe films produced from solutions with $C_{sac} > 0.3 \text{ g L}^{-1}$, an insignificant difference in H_c is observed ($H_c \approx \text{const}$). Additional practical insight from these results is achieved when the H_c values are plotted as functions of the corresponding sulfur incorporation rates (bottom) and the ratio between R_S/R_0 (top, Fig. 4B). Now, it is obvious that the higher incorporation rates of sulfur lead to the 2.4 T CoFe alloys with lower H_c values. This dependence can be fitted with the linear regression with slope of $-34 \times 10^{11} \text{ Oe/mol cm}^{-2} \text{ s}^{-1}$, shown as a dashed line in Fig. 4B. Further practical information obtained from this analysis is that in order to decrease the coercivity of the 2.4 T CoFe alloys produced without additives in the plating solution by $\approx 50\%$, the incorporation rate of sulfur with the addition of saccharin has to increase approximately six times. Another important result related to the relative importance of each mechanism to the observed softness of 2.4 T CoFe alloys can be deduced if the coercivity of the 2.4 T CoFe films is plotted as a function of the ratio between the R_M and R_{ER} incorporation rates (Fig. 5). As long as R_M represents the domi-

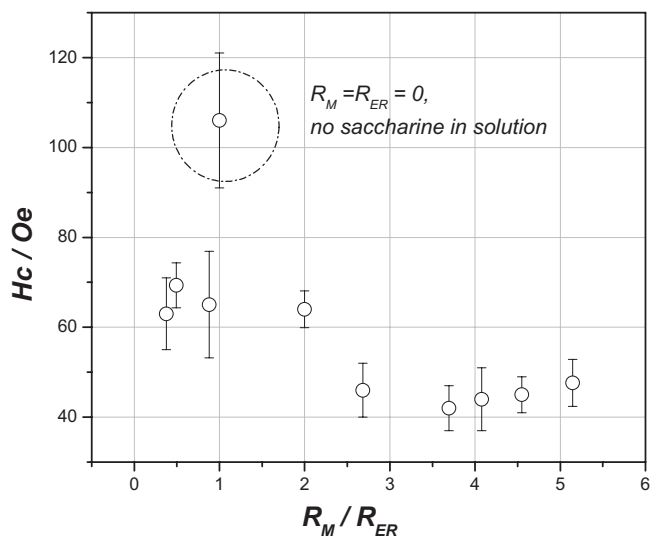


Figure 5. Coercivity of 2.4 T CoFe alloys as a function the R_M/R_{ER} ratio.

nant contribution to the overall sulfur content in the 2.4 T CoFe alloys ($R_M/R_{ER} > 2$), the measured coercivity of the electrodeposited films has the lowest values, between 40 and 50 Oe (Fig. 5). In the case when R_{ER} is $\sim 50\%$ of R_M or it makes the predominant contribution to the sulfur content in the deposit, $R_M/R_{ER} < 1$, the measured coercivity of the 2.4 T CoFe films is significantly higher, above 60 Oe. It is important to keep in mind that CoFe films with $R_M/R_{ER} < 1$ are still softer than the ones electrodeposited without saccharin in the solution ($H_c = 106$ Oe, Fig. 5). On the basis of these observations, we can conclude that the most effective form of incorporated sulfur producing the soft 2.4 T CoFe alloys is the sulfur as a part of saccharin molecule. The incorporated sulfur as a part of the metal sulfides also contributes to the decrease in the CoFe alloy softness, but less effectively. Therefore, the optimum design of the plating solutions for ultimately soft 2.4 T CoFe alloys has to be such that criterion $R_M \gg R_{ER}$ is satisfied.

Corrosion properties vs R_S .— In order to investigate the effect of sulfur incorporation on the corrosion properties of 2.4 T CoFe alloys, the samples were electrodeposited from solution without saccharin and from the ones containing 0.12 and 2 g L⁻¹ of this additive. After the deposition, these samples were carefully rinsed with ultrapure water and submitted to corrosion potential measurements. The results are presented in Fig. 6A. As expected, the noblest CoFe surface with the most positive corrosion potential, $E_c \approx -0.17$ V, is electrodeposited without saccharin in the solution (0.09 at % S). The surface of the CoFe sample electrodeposited from solution containing 0.12 g L⁻¹ of saccharin (0.78 at % S) has the most negative corrosion potential, $E_c \approx -0.6$ V. The sample electrodeposited from the solution containing 2 g L⁻¹ of saccharin (0.43 at % S) has the corrosion potential $E_c \approx -0.3$ V, which is ≈ 0.3 V more positive than in the previous case, indicating higher nobility of this surface. The incorporation rate of sulfur and corresponding S content in the CoFe matrix for the 0.12 g L⁻¹ sample is approximately two times larger than for the 2 g L⁻¹ sample and approximately eight times larger than for the 0 g L⁻¹ sample (Fig. 2). This fact is directly reflected on the corrosion potential of this sample being the most negative, which indicates a significantly poorer corrosion resistance²⁴ (see the inset in Fig. 6A). The anodic linear sweep voltammetry measurements (Fig. 6B) reveal a same trend in electro-oxidation potentials of these samples. The most positive electro-oxidation potential is observed for the 0 g L⁻¹ sample ($E_{ox} \approx -0.3$ V), and then for the 0.2 g L⁻¹ sample ($E_{ox} \approx -0.48$ V), and for the 0.12 g L⁻¹ sample ($E_{ox} \approx -0.55$ V). Our electrochemical impedance measurements (data not shown) performed on these

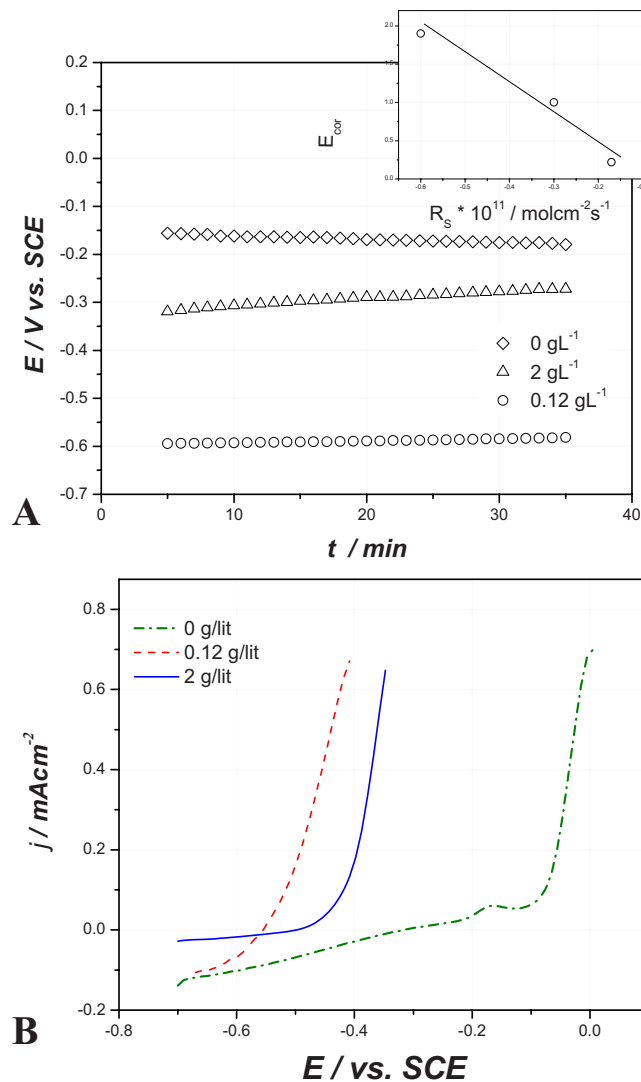


Figure 6. (Color online) (A) Corrosion potential transients for 2.4 T CoFe films electrodeposited from solutions containing 0, 0.12, and 2 g L⁻¹ of saccharin. The inset shows corrosion potential as a function of total sulfur incorporation rate. (B) Linear sweep voltammetry results for 2.4 T CoFe films electrodeposited from solutions containing 0, 0.12, and 2 g L⁻¹ of saccharin. The test solution in both cases is 0.05 M NaCl.

samples are also in agreement with both sets of data in Fig. 6. The largest value of the charge transfer resistance is for the 0 g L⁻¹ sample ($R_{ct} = 10$ k Ω cm⁻²) and then for the 2 g L⁻¹ sample ($R_{ct} = 3.3$ k Ω cm⁻²), while the 0.12 g L⁻¹ sample shows the greatest susceptibility for corrosion indicated by the lowest value of R_{ct} (2.6 k Ω cm⁻²).

All corrosion measurements unambiguously indicate that the samples with higher contents of sulfur and larger sulfur incorporation rates are also the ones that will corrode faster. However, our coercivity measurements show that larger incorporation rates of sulfur lead to softer 2.4 T CoFe alloys (Fig. 4B). It is obvious that the design of the saccharin content in the plating solution has to be done in such a way that both effects are taken into account. In order to evaluate both effects, we propose the dimensionless criterion based on the achieved decrease in coercivity of the CoFe alloys with addition of saccharin in the solution and the corresponding relative increase in CoFe alloy corrosion rate. This criterion is defined as

$$\mathfrak{R} = \frac{H_{c,0}}{H_c(C_{sac})} \frac{j_0}{j(C_{sac})} \quad [11]$$

Here, $H_{c,0}$ and $H_c(C_{\text{sac}})$ stand for coercivities of the CoFe films electrodeposited from solution without and with saccharine, while j_0 and $j(C_{\text{sac}})$ represent the corrosion currents (rates) of the CoFe films electrodeposited from solutions without and with saccharine. The ratio between the corrosion currents [$j_0/j(C_{\text{sac}})$] can be expressed in terms of the difference in the corrosion potentials of these samples as^{30 a}

$$\frac{j_0}{j(C_{\text{sac}})} = \exp\left(-\frac{\alpha F}{RT}\Delta E_{\text{cor}}\right) \quad [12]$$

In Eq. 12, α stands for the transfer coefficient of the reduction reaction occurring on the CoFe surface during corrosion process (oxygen reduction or H^+ ion reduction), while F , R , and T are Faraday's constant, universal gas constant, and absolute temperature, respectively. The value ΔE_{cor} is defined as the difference between corrosion potentials of the samples produced without and with saccharin in the solution [$\Delta E_{\text{cor}} = E_{\text{cor},0} - E_{\text{cor}}(C_{\text{sac}})$]. One should note that more negative corrosion potentials measured for samples produced from saccharin containing solutions result in $\Delta E_{\text{cor}} > 0$ and therefore values of [$j_0/j(C_{\text{sac}})$] < 1 .

In order to evaluate the criterion \mathfrak{R} , the ratio [$H_{c,0}/H_c(C_{\text{sac}})$] has to be obtained from magnetic measurements. Evidently, the addition of saccharin in the solution results in softer CoFe alloys and consequent value of [$H_{c,0}/H_c(C_{\text{sac}})$] is always > 1 . For the 2 and 0.12 g L⁻¹ samples, these values are 1.7 and 2.5. The [$j_0/j(C_{\text{sac}})$] ratio can be calculated using the measured corrosion potentials and taking the oxygen reduction on CoFe surface as the representative reduction reaction ($\alpha = 0.5$ for pH 7).^{31 b} For the 2 and 0.12 g L⁻¹ samples, the calculated current ratios are 0.08 and 0.0003. The \mathfrak{R} criterion is now calculated to be 0.14 (2 g L⁻¹) and 0.00075 (0.12 g L⁻¹). The values of \mathfrak{R} being < 1 for both samples indicate that the gain achieved by decrease in coercivity of the CoFe alloys is much smaller than the corresponding increase in their corrosion rates. Ideally, the right choice of additive and design of its content in the plating solution would be the one that yields \mathfrak{R} value ≥ 1 . This would mean that the decrease in coercivity of the sample produced with additive in solution is many times greater than the corresponding increase in its corrosion rate or, in some special cases, that a decrease in coercivity is achieved as well as a decrease in corrosion rate. However, in the case of saccharin as an additive, the \mathfrak{R} values < 1 are always observed for CoFe alloys. For our two samples, it is evident that the $C_{\text{sac}} = 2$ g L⁻¹ solution yields the CoFe films with \mathfrak{R} value that is closer to 1 than the $C_{\text{sac}} = 0.12$ g L⁻¹ solution. Because of that, the 2 g L⁻¹ saccharin concentration represents the better choice when the overall optimum in both corrosion rate and magnetic softness of 2.4 T CoFe films is considered.

Conclusion

In this paper, a comprehensive investigation of sulfur incorporation into 2.4 T CoFe deposits is presented. The results show that saccharin used as an additive is the main source of sulfur in the deposit for C_{sac} between 0.06 and 2.5 g L⁻¹. The sulfur incorporation occurs by three independent mechanisms from which two are related to saccharine: the physical incorporation of saccharin molecules and saccharin electroreduction. An analytical model is developed [Eq. 10], which succeeds to qualitatively describe our experimental data. This model suggests that saccharin molecules are the dominant source of sulfur in the deposit for $C_{\text{sac}} < 0.7$ g L⁻¹. For

$C_{\text{sac}} > 0.7$ g L⁻¹, the dominant source of sulfur in the deposit is metal sulfides. The measured coercivity of electrodeposited 2.4 T CoFe films shows a direct correlation with the incorporation rate of sulfur (content of sulfur in the deposit). The softer the CoFe films are, the greater content of sulfur they have. Our corrosion measurements also show that the incorporation of sulfur into 2.4 T CoFe films leads to their higher corrosion susceptibility. In order to quantify the effect of sulfur incorporation on both magnetic and corrosion properties, a dimensionless criterion is proposed (Eq. 11) that could be used to make a decision about the optimum saccharin concentration in the plating solution.

Acknowledgments

The authors thank Dr. James Meen from Texas Center for Superconductivity for help during WDS measurements. This work is sponsored by DOD, Strategic Environmental Research and Development Program, under contract no. MMI593 and by NSF, Division of Industrial Innovation and Partnership under contract no. IIP0638195.

University of Houston assisted in meeting the publication costs of this article.

References

1. K. G. Ashar, *Magnetic Disk Drive Technology*, IEEE, New York (1997).
2. E. I. Cooper, G. Bonhote, J. Heidmann, Y. Hsu, P. Kem, J. W. Lam, M. Ramasubramanian, N. Robertson, L. T. Romankiw, and H. Xu, *IBM J. Res. Dev.*, **49**, 103 (2005).
3. S. R. Brankovic, X. M. Yang, T. J. Klemmer, and M. Siegler, *IEEE Trans. Magn.*, **42**, 132 (2006).
4. S. R. Brankovic, K. Sendur, T. J. Klemmer, X.-M. Yang, and E. C. Johns, in *Magnetic Materials Processes and Devices VII and Electrodeposition of Alloys*, S. Kröngelb, L. T. Romankiw, J.-W. Chang, K. Kitamoto, J. W. Judy, C. Bonhôte, G. Zangari, and W. Schwarzacher, Editors, PV 27-2002, p. 269, Electrochemical Society Proceeding Series, Pennington, NJ (2002).
5. L. T. Romankiw and D. A. Thompson, U.S. Pat. 4,295,173 (1981).
6. N. Robertson, H. L. Hu, and C. Tsang, *IEEE Trans. Magn.*, **33**, 2818 (1997).
7. I. Tabakovic, S. Reimer, V. Inturi, P. Jalen, and A. Thayer, *J. Electrochem. Soc.*, **147**, 219 (2000).
8. T. Osaka, M. Takai, K. Hayashi, K. Ohashi, M. Saito, and K. Yamada, *Nature (London)*, **392**, 796 (1998).
9. X. Liu, G. Zangari, and M. Shamsuzzoha, *J. Electrochem. Soc.*, **150**, C159 (2003).
10. T. Osaka, T. Yokoshima, D. Shiga, K. Imai, and K. Takashima, *Electrochem. Solid-State Lett.*, **6**, C53 (2005).
11. M. Schlesinger and M. Paunovic, *Modern Electroplating*, John Wiley & Sons, Hoboken, NJ (2000).
12. T. Osaka, T. Sawaguchi, F. Mizutani, T. Yokoshima, M. Takai, and Y. Okinaka, *J. Electrochem. Soc.*, **146**, 3295 (1999).
13. B. N. Popov, K.-M. Yin, and R. E. White, *J. Electrochem. Soc.*, **140**, 1321 (1993).
14. S. R. Brankovic, N. Vasiljevic, T. J. Klemmer, and E. C. Johns, *J. Electrochem. Soc.*, **152**, C196 (2005).
15. J. Edwards, *Trans. Inst. Met. Finish.*, **39**, 52 (1962).
16. S. R. Brankovic, F. Wiatrowski, and M. Siegler, abstract 473, p. 208, ECE Meeting, Quebec City, May 15, 2005.
17. S. R. Brankovic, R. Haislmaier, and N. Vasiljevic, *Electrochem. Solid-State Lett.*, **10**, D67 (2007).
18. G. S. Frankel, V. Brusica, R. G. Schad, and J.-W. Chang, *Corros. Sci.*, **35**, 63 (1993).
19. T. Osaka, M. Takai, T. Y. Sogawa, T. Momma, K. Ohashi, M. Saito, and K. Yamada, *J. Electrochem. Soc.*, **146**, 2092 (1999).
20. I. Tabakovic, S. Reimer, K. Tabakovic, M. Sun, and M. Kief, *J. Electrochem. Soc.*, **153**, C586 (2006).
21. L. Ricq, F. Lallemand, M. P. Gigandet, and J. Pagetti, *Surf. Coat. Technol.*, **138**, 278 (2001).
22. F. Lallemand, L. Ricq, P. Bercot, and J. Pagetti, *Electrochim. Acta*, **47**, 4149 (2002).
23. S. R. Brankovic, R. Haislmaier, and N. Vasiljevic, *ECS Trans.*, **3**, 71 (2007).
24. U. R. Evans, *An Introduction to Metallic Corrosion*, p. 32, 248, ASM-Edward Arnold, London (1982).
25. K.-M. Yin, *J. Electrochem. Soc.*, **150**, C435 (2003).
26. V. G. Levich, *Physicochemical Hydrodynamics*, Prentice-Hall, Englewood Cliffs, NJ (1962).
27. J. M. Smith, *Chemical Engineering Kinetics*, 2nd ed., p. 283, McGraw Hill, New York (1970).
28. C. H. Hamann, A. Hamnett, and W. Vielstich, *Electrochemistry*, p. 187, Wiley-VCH, New York (1998).
29. W. Bang and K. Hong, *Electrochem. Solid-State Lett.*, **10**, J86 (2007).
30. G. Prentice, *Electrochemical Engineering Principles*, p. 143, Prentice Hall, Englewood Cliffs, NJ (1991).
31. V. Jovancevic and J. O'M. Bockris, *J. Electrochem. Soc.*, **133**, 1799 (1986).

^a To derive the expression for the currents ratio we assume that no transport limitations and that at a given corrosion potentials the kinetics of this half cell corrosion reaction is well described by Tafel approximation. For more details, see, for example, Ref. [30]

^b At pH 7, the dominant reduction reaction on CoFe surface during the corrosion process is oxygen reduction. The $\alpha = 0.5$ corresponds to the Tafel slope of 120 mV/decade, which is commonly measured during oxygen reduction on bare Fe surface at pH 7. See, for example, Ref. [31]